Calcif Tissue Int (2016) 98:263–274
DOI 10.1007/s00223-015-0085-3

ORIGINAL RESEARCH

Effects of Sclerostin Antibody on the Healing of Femoral Fractures in Ovariectomised Rats

Yang Liu[1] · Yunfeng Rui[1] · Tin Yan Cheng[4] · Shuo Huang[1] · Liangliang Xu[1] · Fanbiao Meng[1] · Wayne Yuk Wai Lee[1] · Ting Zhang[1] · Nan Li[4] · Chaoyang Li[3] · Huazhu Ke[3] · Gang Li[1,2,4,5]

Received: 11 September 2015 / Accepted: 10 November 2015 / Published online: 24 November 2015

Abstract The inhibition of sclerostin by the systemic administration of a monoclonal antibody (Scl-Ab) significantly increased bone mass and strength in fractured bones in animal models and non-fractured bones in ovariectomised (OVX) rats. In this study, the effects of Scl-Ab on healing were examined in a closed fracture model in OVX rats. Sixty Sprague-Dawley rats underwent an ovariectomy or a sham operation at 4 months of age, and a closed fracture of the right femur was performed 3 months later. Subcutaneous injections with Scl-Ab (25 mg/kg) or saline were then administered on day 1 after the fracture and twice a week for 8 weeks ($n = 20$ per group), at which time the fractured femurs were harvested for micro-computed tomography analysis, four-point bending mechanical testing and histomorphometric analysis to examine bone mass, bone strength and dynamic bone formation at the fracture site. The angiogenesis at the fracture site was also examined. Bone marrow stem cells were also isolated from the fractured bone to perform a colony-forming unit (CFU) assay and an alkaline phosphatase-positive (ALP^+) CFU assay. OVX rats treated with Scl-Ab for 8 weeks had significantly increased bone mineral density and relative bone volume compared with OVX rats treated with saline. Similarly, maximum loading, energy to maximum load and stiffness in Scl-Ab-treated OVX rats were significantly higher than those in saline controls. The mineral apposition rate (MAR), mineralising surface (MS/BS) and bone formation rate (BFR/BS) were also significantly increased in Scl-Ab-treated group compared with the saline-treated group in OVX rats. Furthermore, the Scl-Ab-treated group had more CFUs and ALP^+ CFUs than the saline-treated group in OVX rats. No significant difference in angiogenesis at the fracture site was found between the groups. Our study demonstrated that Scl-Ab helped to increase bone mass, bone strength and bone formation at the fracture site in a closed femoral fracture model in OVX rats. Bone marrow stem cells in OVX rats injected with Scl-Ab also had increased CFUs and ALP^+ CFUs.

Keywords Fracture healing · Ovariectomy · Sclerostin antibody

Yang Liu and Yunfeng Rui contributed equally to this work.

✉ Gang Li
gangli@cuhk.edu.hk

1 Department of Orthopaedics and Traumatology, Faculty of Medicine, Li Ka Shing Institute of Health Sciences, The Chinese University of Hong Kong, Prince of Wales Hospital, Hong Kong, China

2 Stem Cells and Regenerative Medicine Laboratory, Lui Che Woo Institute of Innovative Medicine, Li Ka Shing Institute of Health Sciences, The Chinese University of Hong Kong, Prince of Wales Hospital, Hong Kong, China

3 Department of Metabolic Disorders, Amgen Inc., Thousand Oaks, California, USA

4 Key Laboratory for Regenerative Medicine, Ministry of Education, School of Biomedical Sciences, Faculty of Medicine, The Chinese University of Hong Kong, Hong Kong, China

5 The CUHK-ACC Space Medicine Centre on Health Maintenance of Musculoskeletal System, The Chinese University of Hong Kong Shenzhen Research Institute, Shenzhen, China

Introduction

Osteoporotic fractures are highly prevalent, occurring in about 40–50 % of women and 13–22 % of men during their lifetime and creating a significant public health

problem [1, 2]. The remodelling of normal bone is mediated by the coordinated actions of osteoclasts (bone resorbing) and osteoblasts (bone forming) [3–5]. An imbalance in bone remodelling—with the rate of bone resorption (mediated by osteoclasts) being higher than that of bone formation (mediated by osteoblasts)—will cause bone loss and a greater fragility of osteoporotic bone [6]. Due to the low bone mineral density (BMD), decreased bone strength and increased fragility of osteoporotic bone, osteoporotic fractures are associated with a high risk of delayed union, non-union and other complications [7].

Canonical Wnt signalling—or the Wnt/β-catenin pathway—is known to play an important role in the healing of fractures [8–11]. Sclerostin, which is an inhibitor of the Wnt signalling pathway and a glycoprotein secreted by osteocytes, has been shown to be a key negative regulator of bone mass and bone formation [6, 12, 13]. Mechanistically, sclerostin has been shown to bind with LRP5/6, a Wnt co-receptor, to inhibit Wnt binding and signalling and decrease bone formation [3, 14, 15]. Previous studies also confirmed the reverse relationship between sclerostin and bone mass. Patients with sclerosteosis, caused by mutations of the *SOST* gene, had markedly increased bone mineral density at all skeletal sites including the lumbar spine, total hip and forearm [16, 17], while the over-expression of the *SOST* gene in transgenic mice can lead to osteopenia [18]. Furthermore, the systemic administration of a monoclonal sclerostin antibody (Scl-Ab) can significantly increase bone mass and bone strength in both intact bones and fractured bones in many animal models [3, 19]. Recent studies have shown that Scl-Ab can help to increase bone mass in postmenopausal women and ovariectomised (OVX) rats [6, 20]. Taken together, we hypothesised that Scl-Ab may also help to promote the healing of fractures in OVX rats by increasing bone mass, bone strength and bone formation at the fracture site.

In our study, we used the OVX rat model recommended by the Food and Drug Administration to establish osteopenia [6]. The rat model of closed femoral fractures was chosen to study the physiological process of fracture for its minimal comminution and angulation of the intramedullary pin and minimal soft tissue damage [21]. We examined the effects of Scl-Ab on the healing of fractures in OVX rats by assessing bone mass using micro-computed tomography (CT) scanning, dynamic bone formation through histomorphometric analysis, bone strength at the fracture site by mechanical testing and angiogenesis by micro-CT-based angiography. The colony-forming unit (CFU) assay and the alkaline phosphatase-positive (ALP^+) CFU assay were also performed to study the underlying mechanisms.

Methods

Details of Animals and Groups

Sixty female Sprague-Dawley rats were obtained from the Laboratory Animal Services Centre of the Chinese University of Hong Kong and were randomised to receive an ovariectomy or a sham operation at 4 months of age (OVX surgery = 40 rats, sham surgery = 20 rats). At 3 months after the operation, a closed fracture of the right femur was performed. On day 1 after the fracture, OVX rats received a subcutaneous injection of 25 mg/kg of Scl-Ab (20 rats) or saline (20 rats), and sham rats were injected with saline (20 rats; control group) and injections were subsequently performed twice a week for 8 weeks. Rats were housed in plastic cages at 25 ± 1 °C and constant humidity, with a standard 12:12 h light/dark cycle beginning at 11.00 am, and were fed a standard laboratory chow and sterile water ad libitum. Ethics approval was obtained for this animal experiment from the Ethics Committee of the Chinese University of Hong Kong.

The current study involved two experimental groups (OVX–Saline, OVX-Scl-Ab) and one control group (Sham–Saline). Prior to the fracture, the proximal tibia of five rats from each group was scanned using a micro-CT (viva CT 40; Scanco Medical, Bassesdorf, Switzerland) to confirm the establishment of osteoporosis induced by the ovariectomy. High-resolution digital radiography (Faxitron MX-20; Faxitron X-ray, Illinois, USA) was carried out weekly to monitor the healing of the fracture. All rats were euthanised 8 weeks after the fracture (at 9 months of age), and the fractured femurs were harvested for micro-CT analysis ($n = 8$ per group), four-point bending mechanical testing ($n = 12$ per group; H25KS; Hounsfield Test Equipment, UK) and histological examination to determine bone mass, bone strength and dynamic bone formation at the fracture site.

Animal Surgery

Ovariectomies or sham operations were performed on female rats at 4 months of age and all rats were held with no further treatment for 3 months to allow the development of osteoporotic changes. The osteoporotic development was confirmed by comparing the bone mineral density (BMD) and trabecular parameters at the proximal tibia through micro-CT scanning. At 7 months of age, a closed fracture of the right femur was performed on all rats. Briefly, the fracture was performed under general anaesthesia with intraperitoneal injections of ketamine hydrochloride (75 mg/kg) and xylazine (10 mg/kg). The blunt dissections were made along the medial side of the

patellar tendon, and then, the patellar bone was dislocated to expose the articular surface of the femoral condyle. A sterilised Kirschner wire (Φ 1.2 mm) was inserted into the femoral medullary canal through the intercondylar notch, and the proximal side of the femur was perforated. The Kirschner wire was bent at the proximal femur to prevent dislocation and cut at the articular surface of the distal femur to allow free joint movement. After suturing, the rats were positioned supinely on a customised three-point bending machine. The closed fracture of the midshaft of the femur was created by dropping a metal blade (weighing 500 g) from a height of 35 cm. The fracture was confirmed by digital radiography with an obvious fracture gap or displacement. From day 1 after fracture surgery, the rats were administered temgesic (0.03 mg/kg) subcutaneously for three consecutive days for pain relief.

Measurement of Body Weight

Body weight was measured on the day of the ovariectomy (baseline), the day of the femoral fracture 3 months later after the ovariectomy (week 0), during treatment with Scl-Ab at week 4 and at the termination of the experiment at week 8.

Micro-CT Analysis of Osteoporotic Development

To confirm the effects of the OVX model, the right proximal tibia was scanned by micro-CT in vivo (viva CT 40; Scanco Medical) at a voltage of 70 keV with a current of 114 μA at week 0, week 4 and week 8 after fracture surgery. The right hind limbs were placed into a plastic cylindrical holder under anaesthesia (3 % isoflurane). The region of proximal tibia was scanned from the growth plate distally to 7.98 mm with a voxel size of 19 μm (420 slices). From this region, a series of slices beginning at a proximal distance of 0.5 mm from the higher end of the growth plate and a length of 1.5 mm were chosen for the evaluation. To separate the trabecular bone from the cortices, the inner trabecular bone was segmented using semi-automatic contours (inner value = 50, outer value = 500). A three-dimensional (3D) reconstruction of the trabecular bone was performed using the selected slices with a low-pass Gaussian filter (sigma = 1.2, support = 2 and threshold = 190). After the 3D reconstruction, the trabecular number (Tb.N), trabecular thickness (Tb.Th), trabecular separation (Tb.Sp) and BMD were evaluated by the built-in software [22].

Micro-CT Analysis of Fractured Bone

To compare the BMD of the fracture zone, the intramedullary Kirschner wire and surrounding soft tissues were first removed. All the femoral samples were then scanned by micro-CT system (viva CT 40; Scanco Medical) at a voltage of 70 keV and a current of 114 μA. The scanned callus region covered 4.326 mm proximally and 4.326 mm distally to the fracture line with a voxel size of 21 μm (412 slices). The contoured regions of interest (ROIs) were selected from 2D CT images covering the whole 412 slices. 3D reconstructions of the mineralised tissues were performed using a low-pass Gaussian filter (sigma = 1.2, support = 2) with the same threshold (attenuation = 190). The following morphometric parameters were evaluated by the built-in software: relative bone volume (BV/TV) and BMD.

Mechanical Testing

The mechanical properties of the femurs were examined 8 weeks after the fracture using a four-point bending test. Before mechanical testing, the femurs were taken out of the freezer and thawed overnight at an air-conditioned room temperature of 22 °C. A material test machine (H25KS; Hounsfield Test Equipment) with a 250 N load cell was used to test the femur for failure. During the mechanical testing, the femurs were placed horizontally with the anterior surface upwards, and centred on the supports at a distance of 10 mm. The load was constantly applied at the fracture site with a displacement rate of 5 mm/min and was directed vertically to the midshaft with the anterior surface upward. After failure of the bone, the following parameters were calculated by the built-in software (QMAT Professional; Tinius Olsen, Horsham, PA, USA): maximal loading, energy to maximal loading (energy) and stiffness.

Histomorphometric Analysis

Sequential fluorescent labelling was used to study the dynamic bone formation during the healing of the fracture. At 14 days prior to euthanasia, 10 mg/kg calcein green was injected subcutaneously into three rats from each group. In addition, 90 mg/kg xylenol orange was injected subcutaneously 10 days prior to euthanasia into the same rats. The difference between the two dyes clearly denoted the dynamic bone formation [23]. During sample collection, the femora were prepared for undecalcified histomorphometry according to an established protocol [24]. Briefly, the femora were dehydrated serially in alcohol and xylene, and were embedded in methyl methacrylate. The embedded samples were sectioned sagittally by a saw microtome (Leica SP1600; Leica, Nussloch, Germany), ground and polished to 100 μm before analysis. The fluorochrome-labelled sections of the femur were examined under a fluorescent microscope (Leica DMRXA2; Leica). Histomorphometric analyses were conducted using the Osteomeasure bone analysis software (Osteometrics,

Decatur, GA, USA). The ROIs were standardised within the external callus region located 2.0 mm proximally or distally to the fracture line. In each group, two sections from each of three rats were examined. The mineral apposition rate (MAR), mineralising surface (MS/BS) and bone formation rate (BFR/BS) were calculated and expressed according to the published methods [6, 24].

Vascular Perfusion and Sample Decalcification

The vascular perfusion was performed using an established protocol [25]. Briefly, the rats were first anaesthetised with an intraperitoneal injection of ketamine (75 mg/kg) and xylazine (10 mg/kg). The abdominal cavity of the rats was then opened, and a scurf needle was inserted into the abdominal aorta distal to the heart with a ligation of that proximal to the heart. The vasculature was flushed with heparinised normal saline (100 U/mL) at 37 °C, and a flow speed was maintained at 20 mm/min via an automatic pump apparatus (PHD 22/2000; Harvard Apparatus, USA) linked to the syringe. As soon as the outflow from an incision of the abdominal vein was limpid, 10 % neutral buffered formalin (37 °C) was pumped into the vasculature to fix the nourished skeletal specimen. When the formalin was flushed from the vasculature using heparinised saline, it was then injected with Microfil (Microfil MV-122; Flow Tech, Carver, MA, USA), a lead chromate-containing confected radiopaque silicone rubber compound, based on the manufacturer's protocol. To ensure polymerisation of the contrast agent, the carcasses were stored at 4 °C for 24 h. Both femurs were then harvested and fixed at 4 °C for 48 h in 10 % neutral buffered formalin, and then transferred to a 9 % formic acid solution to decalcify the mineralised bone. Successful decalcification was confirmed by anteroposterior view radiographs taken using a cabinet X-ray system (Specimen Radiography System, Faxitron; Faxitron X-ray Corporation) under an exposure condition of 40 kV/30 s. The decalcified samples were stored in 10 % neutral buffered formalin until micro-CT scanning.

Micro-CT Analysis for Angiogenesis

To compare the density of the micro-angiography at the fracture region, the harvested femoral samples were placed into a sample tube with the long axis perpendicular to the bottom of the tube for CT scanning using a viva CT 40 (Scanco Medical) with a voltage of 70 keV and a current of 114 μA. The scanned region covered 4.33 mm proximally and 4.33 mm distally to the fracture line with a voxel size of 21 μm. The contoured ROIs were selected from 2D CT images covering the whole 412 slices. To segment the blood vessels from background, noise was removed using a low-pass Gaussian filter (sigma = 1.2, support = 2) with the same threshold (attenuation = 240). The following parameters were evaluated by built-in software: vessel volume, vessel diameter and vessel volume fraction [26].

Isolation of Rat Bone Marrow Stem Cells (BMSCs)

BMSCs were isolated as described previously [27]. Briefly, at week 8 after the fracture, three femurs from each group were removed and rinsed in sterilised phosphate buffered saline (PBS). The proximal femurs were cut off and surrounding muscles were dissected. Bone marrow tissues were collected by flushing out through the intercondylar fossa with an 18G needle and rinsed in PBS. The mononuclear cells were isolated with Lymphoprep (Stem Cell Technologies, Canada) after density gradient centrifugation (1000 g, 30 min) and re-suspended in culture medium containing alpha minimum essential medium (α-MEM; Gibco), 10 % fetal bovine serum, 100 U/mL of penicillin, 100 μg/mL of streptomycin and 2 mM L-glutamine (Invitrogen, USA). Cells were plated at a low density of 100 cells per 10-cm^2 dish and cultured for 10 days, with the medium being renewed every 3 days. Cultures were performed in triplicate.

Colony-Forming Unit (CFU) Assay and Alkaline Phosphatase-Positive (ALP^+) CFU assay

After 10 days of culture, the cells were stained with 0.5 % crystal violet (Sigma, St Louis, MO, USA) to count the number of cell colonies. A 5-bromo-4-chloro-3-indolyl phosphate and nitro blue tetrazolium substrate (Promega, USA) was used to perform the ALP staining. Colonies visualised as dark blue were considered to be formed by BMSCs, while those smaller than 2 mm in diameter and faintly stained were ignored.

Statistical Analysis

All results were expressed as the mean ± standard deviation. The statistical differences among groups were analysed by the analysis of variance least significant difference (ANOVA LSD) post hoc test. Values of $p < 0.05$ were considered to be significant. All analyses were performed using IBM SPSS Statistics 22.

Results

Measurement of Body Weight

The body weights at different time-points are shown in Table 1 and were significantly affected by ovariectomy. No significant difference was found among the groups at the

Table 1 Measurements of body weight

	Sham-Saline	OVX-Saline	OVX-Scl-Ab
Baseline	242.21 ± 12.36	241.14 ± 20.02	240.69 ± 21.26
Week 0	299.62 ± 16.37	347.40 ± 25.94**	357.33 ± 29.68**
Week 4	292.15 ± 18.17	334.70 ± 23.49**	343.75 ± 25.40**
Week 8	292.77 ± 18.94	342.4 ± 24.99**	350.87 ± 27.61**

The data are expressed as the mean ± standard deviation

** $p < 0.01$ vs. Sham–Saline group at the same time

beginning of the experiment at 4 months of age (baseline, $p > 0.05$). Three months after surgery, the body weight of the OVX–Saline group was significantly increased compared with the Sham–Saline group (+18 %, $p < 0.01$). No significant difference was found between the OVX–Saline and OVX-Scl-Ab group at week 0. At week 4 and week 8 after the fracture surgery, the body weights of the OVX–Saline and OVX-Scl-Ab groups were significantly higher than those of the Sham–Saline group (+15 %, $p < 0.01$ and +18 %, $p < 0.01$ at week 4; +17 %, $p < 0.01$ and +20 %, $p < 0.01$ at week 8), respectively. No significant difference between the OVX–Saline group and the OVX-Scl-Ab group was observed at week 4 and week 8 ($p > 0.05$). In addition, no significant difference was found within groups across time-points ($p > 0.05$).

Micro-CT Analysis for Osteoporotic Development

Before and during treatment with Scl-Ab, BMD and trabecular parameters at the proximal region were measured in each group by micro-CT analysis to 1) confirm the establishment of osteoporosis in OVX rats at week 0 and 2) compare the osteoporotic development during treatment at week 4 and week 8 (Fig. 1). At week 0, a significant decrease in BMD (−44 %, $p < 0.001$), Tb.N (−53 %, $p < 0.001$), Tb.Th (−28 %, $p < 0.01$) and 1/Tb.Sp (−64 %, $p < 0.01$) was observed in the OVX groups (OVX–Saline and OVX-Scl-Ab groups) compared with the Sham–Saline group. At week 4 and week 8, the OVX–Saline group also showed a significant decrease in BMD, Tb.N and 1/Tb.Sp compared with the Sham–Saline group, indicating that the oestrogen deficiency bone loss had been successfully established 3 months after ovariectomy. After treatment with Scl-Ab for 4 weeks, the OVX-Scl-Ab group showed a significant increase in Tb.Th (+25 %, $p < 0.05$) and a non-significant increase in BMD (+36 %, $p > 0.05$), Tb.N (+7 %, $p > 0.05$) and 1/Tb.Sp (+11 %, $p > 0.05$) compared with the OVX–Saline group. At week 8, a significant increase in Tb.Th (+47 %, $p < 0.01$) and a non-significant increase in BMD (+59 %, $p > 0.05$), Tb.N (+9 %, $p > 0.05$) and 1/Tb.Sp (+1 %, $p > 0.05$) were observed in the OVX-Scl-Ab group compared with the OVX–Saline group. In addition, after treatment with Scl-Ab for 8 weeks, the OVX-Scl-Ab group showed a significant increase in Tb.Th (+50 %, $p < 0.01$) at week 8 compared with that at week 0, while Tb.Th was significantly decreased in the Sham–Saline group at week 4 and week 8 compared with that at week 0 (−28 %, $p < 0.05$ at week 4; −25 %, $p < 0.05$ at week 8). These results indicated that treatment with Scl-Ab helped to increase bone mass in OVX rats, mainly through the thickness of the trabecular bone.

Micro-CT Analysis for Fracture Bone

Bone mass was measured at the fracture region by micro-CT analysis after treatment with Scl-Ab for 8 weeks. As shown in Fig. 2, the reconstructed mineralised calluses showed different morphological characteristics among the groups in 3D micro-CT images (Fig. 2b). The fracture region showed loose bone morphology in the OVX–Saline group compared with the Sham–Saline group, while more bones were formed in the OVX-Scl-Ab group compared with the OVX–Saline group. The OVX–Saline group also had a large gap at the callus region compared with the Sham–Saline and OVX-Scl-Ab groups. Quantitatively, measurements of BV/TV and BMD were significantly ($p < 0.001$) higher in the OVX-Scl-Ab group than in the OVX–Saline group (+29 % and +28 %, respectively, in Fig. 2c). Moreover, the OVX–Saline group showed a significant ($p < 0.001$) decrease in BV/TV (−22 %) and BMD (−22 %) compared with the Sham–Saline group. No significant difference in BV/TV and BMD was found between the Sham–Saline group and OVX-Scl-Ab groups ($p > 0.05$). These results indicated that OVX rats experienced a delayed healing process of the fracture, while treatment with Scl-Ab helped to promote healing in OVX rats through an increase in bone mass at the fracture region.

Mechanical Testing

To access the bone strength at the fracture region, mechanical testing was performed at week 8. The results are shown in Fig. 2d. The OVX–Saline group showed a non-significant difference in maximal loading (−6 %, $p > 0.05$), energy to maximal loading (+31 %, $p > 0.05$) and stiffness (−26 %, $p > 0.05$) compared with the Sham–Saline group, while the OVX-Scl-Ab group showed a significant increase in maximal loading (+56 %, $p < 0.01$), energy to maximal loading (+82 %, $p < 0.05$) and stiffness (+38 %, $p < 0.05$) compared with the OVX–Saline group. Furthermore, the OVX-Scl-Ab group also showed a significant increase in maximal loading (+46 %, $p < 0.05$) and energy to maximal loading (+138 %, $p < 0.01$) compared with the Sham–Saline group.

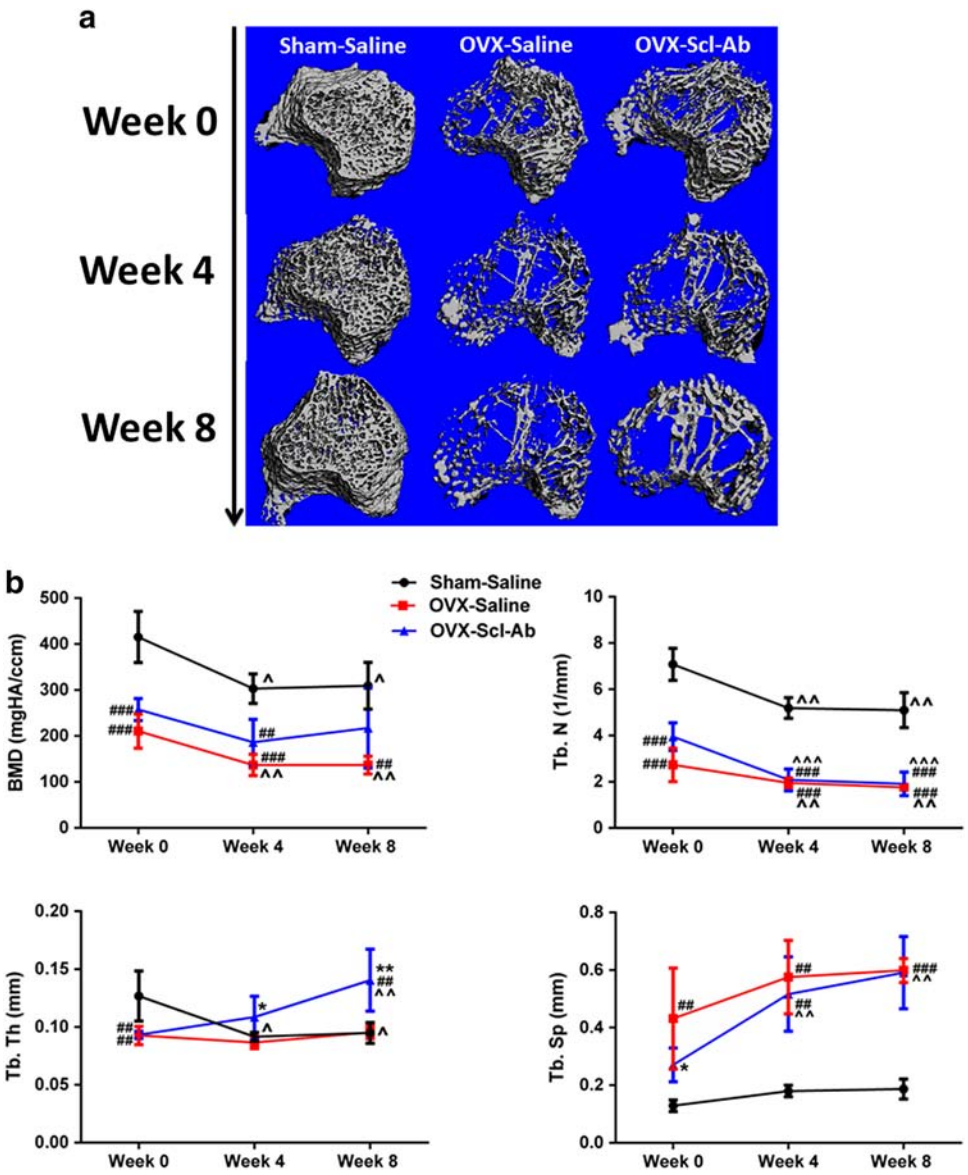

Fig. 1 Micro-CT analysis of osteoporotic development. **a** 3D reconstruction of proximal tibias at week 0, week 4 and week 8 in the four groups. **b** Data analysis of BMD, trabecular number (Tb.N), trabecular thickness (Tb.Th) and trabecular separation (Tb.Sp) of proximal tibias during 8 weeks of treatment among the groups (*$p < 0.05$ vs. OVX–Saline group at the same time point; **$p < 0.01$ vs. OVX–Saline group at the same time; ***$p < 0.001$ vs. OVX–Saline group at the same time; $^{\#}p < 0.05$ vs. Sham–Saline group at the same time point; $^{\#\#}p < 0.01$ vs. Sham–Saline group at the same time point; $^{\#\#\#}p < 0.001$ vs. Sham–Saline group at the same time point; $^{\wedge}p < 0.05$ vs. week 0 in the same group; $^{\wedge\wedge}p < 0.01$ vs. week 0 in the same group)

No significant difference in stiffness was found between the OVX-Scl-Ab and Sham–Saline groups ($p > 0.05$).

Histomorphometric Analysis

We further analysed dynamic bone formation in the periosteal callus region at week 8, and the results are shown in Fig. 3. The OVX-Scl-Ab group showed a significant increase in MS/BS (+43 %, $p < 0.05$) and non-significant increase in BFR/BS (+26 %, $p > 0.05$) and MAR (+22 %, $p > 0.05$) compared with the OVX–Saline group. In addition, the MAR, MS/BS and BFR/BS were also significantly increased in the OVX-Scl-Ab group compared with the Sham–Saline group (+42 %, $p < 0.01$; +69 %, $p < 0.05$; +92 %, $p < 0.05$). No significant difference in the MS/BS, BFR/BS and MAR was found between the Sham–Saline and OVX–Saline groups.

Fig. 2 Sclerostin antibody increases bone mass and bone strength of fracture region after 8 weeks of treatment. **a** A radiograph of closed femoral fracture immediately after surgery. **b** 3D reconstruction images of fracture region at week 8 in the four groups, images in *lower side* show the fracture region cut through the mid-vertical line. **c** Data analysis of BMD and relative bone volume (BV/TV) of fracture region at week 8. **d** Data analysis of the mechanical testing at the fracture region (*$p < 0.05$ vs. OVX–Saline group; **$p < 0.01$ vs. OVX–Saline group; ***$p < 0.001$ vs. OVX–Saline group; $^{\#}p < 0.05$ vs. Sham–Saline group; $^{\#\#}p < 0.01$ vs. Sham–Saline group; $^{\#\#\#}p < 0.001$ vs. Sham–Saline group)

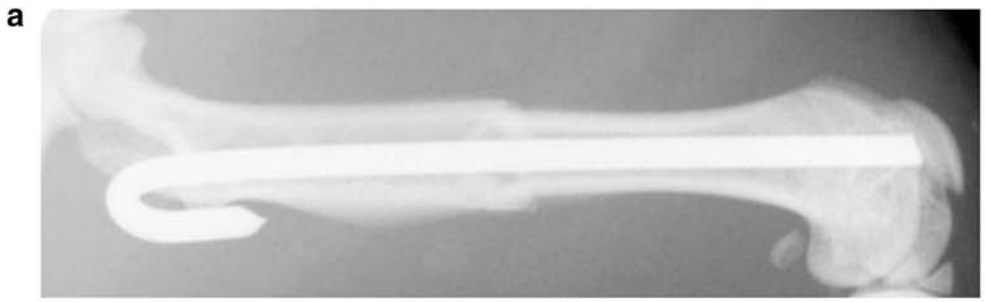

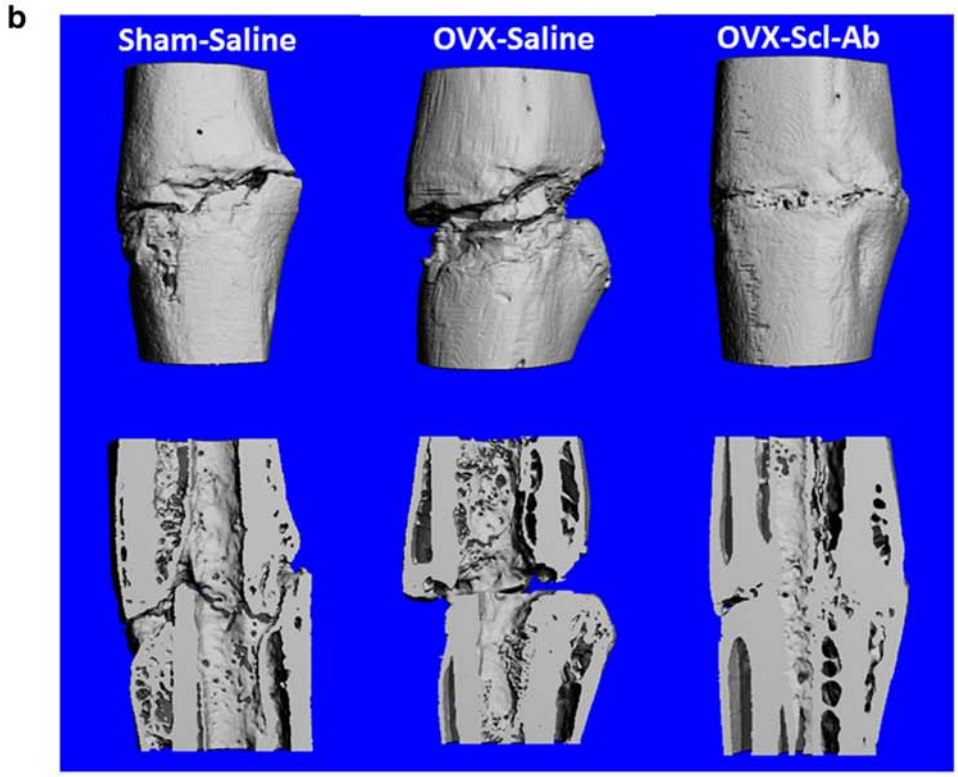

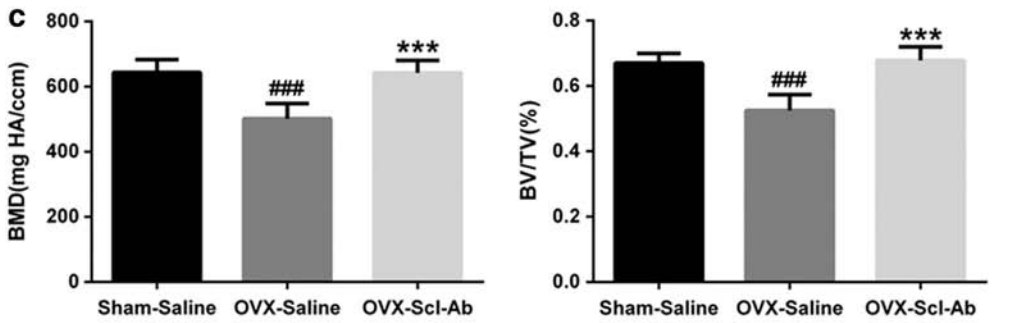

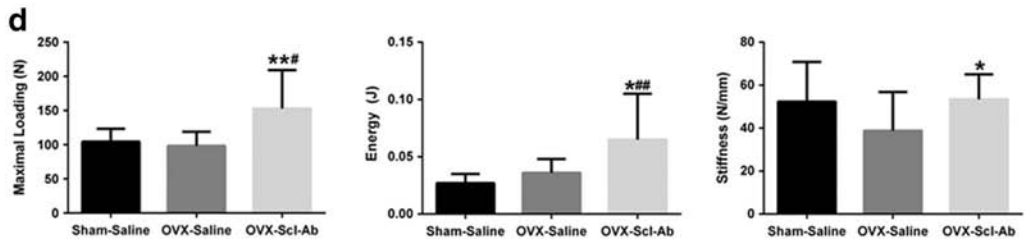

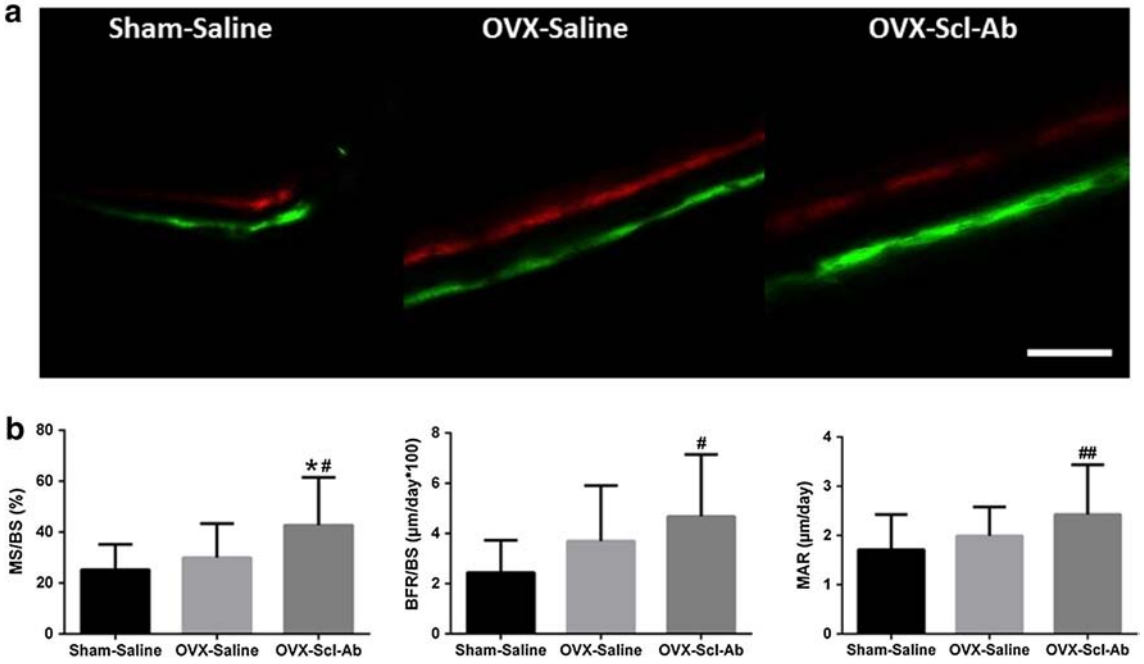

Fig. 3 Sclerostin antibody promotes bone formation during fracture healing. **a** Fluorescent images taken from unstained sections. Calcein green (*green label*) was injected 14 days prior to euthanasia, and xylenol orange (*red label*) was injected 4 days before euthanasia. **b** Average MS/BS, BFR/BS and MAR at fracture region in 10 days during fracture healing (scale bar = 25 μm; $^{*}p < 0.05$ vs. OVX–Saline group; $^{\#}p < 0.05$ vs. Sham–Saline group; $^{\#\#}p < 0.01$ vs. Sham–Saline group) (Color figure online)

Micro-CT analysis for angiogenesis

Angiogenesis was also studied at week 8 to examine the vessel formation during fracture healing by micro-CT analysis (Fig. 4). At week 8 after the fracture, the 3D reconstruction images showed that only a small amount of vessel network was formed in the region of the fracture in each group. Most newly formed vessels were less than 0.10 mm (in green colour) in diameter in each group. No significant difference in the measurements of total vessel volume, vessel volume diameter and vessel volume fraction was found between groups ($p > 0.05$).

CFU Assay and ALP^{+} CFU Assay

As sclerostin is expressed on osteocytes that can reduce the differentiation of BMSCs into osteoblasts, whether Scl-Ab could promote osteogenesis by increasing the activity of BMSCs had yet to be elucidated. To evaluate this, the CFU and ALP^{+} CFU activities were measured. As shown in Fig. 5, more colonies were formed in the OVX-Scl-Ab group, and the number of colonies in each well was significantly higher than that of either the OVX–Saline or Sham–Saline groups ($p < 0.01$, Fig. 5a). The number of ALP^{+} CFUs per well in the OVX-Scl-Ab group was also significantly higher than that in the OVX–Saline and Sham–Saline groups ($p < 0.05$, Fig. 5b).

Discussion

Patients with osteoporotic fractures may experience delayed union or non-union due to low bone mass and other factors [7, 28]. The inhibition of sclerostin by systemic administration of Scl-Ab has been shown to increase bone mass and promote the healing of fractures in animal models of fracture repair [3, 29]. In this study, we performed a closed femoral fracture on rats with established osteopenia induced by ovariectomy to examine the effects of Scl-Ab on fracture healing in OVX rats. Our results demonstrated that Scl-Ab enhanced fracture healing in OVX rats by improving bone mass, bone strength and bone formation at the fracture region compared with OVX rats injected with saline. Moreover, Scl-Ab treatment of OVX rats also resulted in a complete reversal of the levels of bone mass and bone strength compared with the Sham–Saline group during fracture healing.

We first performed an ovariectomy on rats to establish an animal model of osteoporosis. The overall data in Table 1 and Fig. 1 indicated that the oestrogen deficiency-induced bone loss had been well established. In the OVX model, the thickness of the trabecular bone at the proximal tibia was dramatically increased after Scl-Ab treatment, as the Tb.Th was significant increased (+50 %) at week 8 compared with that at week 0 in the OVX-Scl-Ab group, which also indicated that Scl-Ab helped to increase bone

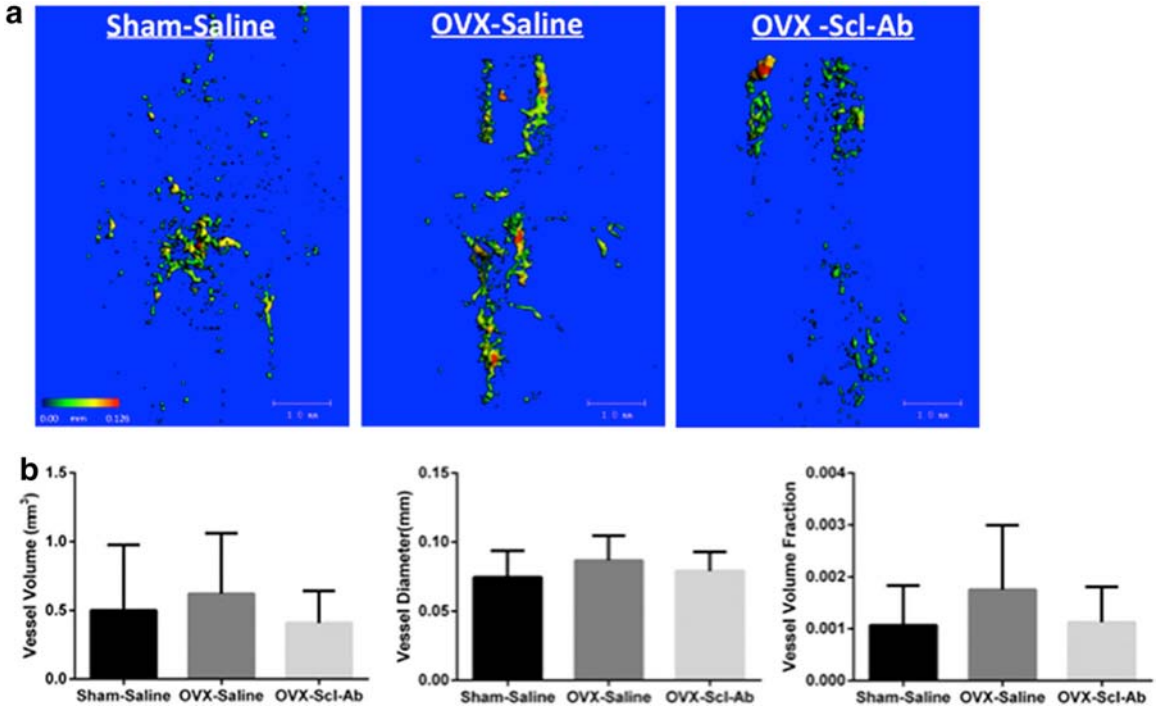

Fig. 4 Micro-CT analysis of angiogenesis at week 8. **a** 3D reconstruction images of angiogenesis at fracture region. **b** Data analysis of vessel volume, vessel diameter and relative vessel volume of the fracture region at week 8 [*white scale bar* = 1.0 mm; *colour scale bar*: from 0.0 mm (*left in blue*) to 0.126 mm (*right in red*)] (Color figure online)

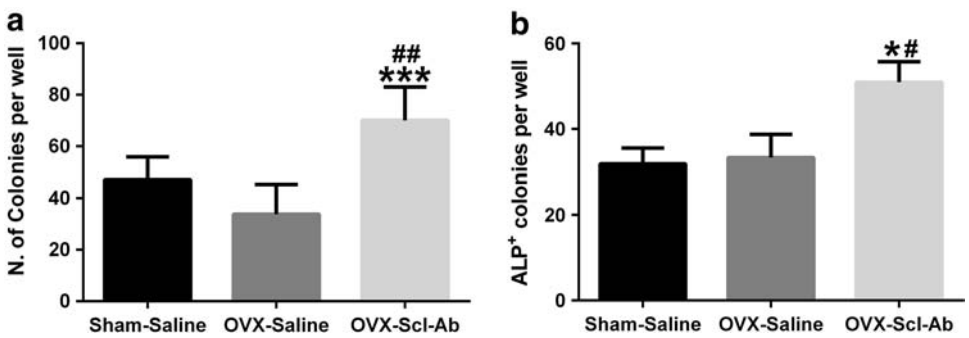

Fig. 5 CFU and ALP^+ CFU analysis of BMSCs. **a** Number of colonies formed of BMSCs after 10 days of culture in each group. **b** ALP^+ CFUs analysis on day 10 after initial culture ($^*p < 0.05$ vs. OVX–Saline group; $^{***}p < 0.001$ vs. OVX–Saline group; $^{\#}p < 0.05$ vs. Sham–Saline group; $^{\#\#}p < 0.01$ vs. Sham–Saline group)

mass in the OVX model, especially in the thickness of bone. Osteoporosis is an imbalance of bone resorption and bone formation [6, 28]. In our study, the injection began 3 months later after the OVX surgery. The OVX rats may still lose bone from week 0 to week 4 after injection (when bone resorption is faster than bone formation), while the bone loss slowed down from week 4 to week 8 (BMD of OVX–Saline group in Fig. 1b). In the OVX-Scl-Ab group, the Scl-Ab may help to promote bone formation after injection, but the bone loss (bone resorption) was still happening during this stage. The rate of bone loss may be faster than the rate of bone formation, hence the BMD in OVX-Scl-Ab group still decreased at week 4. To confirm this notion further, Padhi and colleagues reported that a sclerostin-neutralising monoclonal antibody resulted in a dose-dependent increase in serum bone formation markers in healthy postmenopausal women [30]. However, measurement of bone resorption at the histological level and serum bone turnover markers (e.g., osteopontin, osteocalcin and collagen type 1 cross-linked C-telopeptide) should be explored in future studies. To examine fracture healing, we performed micro-CT to measure bone mass in the fracture region after 8 weeks of treatment (Fig. 2). The micro-CT analysis of the fractured bone showed that Scl-Ab helped to increase bone mass at the fracture site in the OVX models. As indicated in the 3D reconstruction images, more new bone was formed in the OVX-Scl-Ab group than in the OVX–Saline group. The data on BV/TV and

BMD of the fracture region in the OVX-Scl-Ab group also confirmed that Scl-Ab helped to increase bone mass compared with the OVX–Saline group by enhancing endochondral ossification. The remodelling process of the periosteal callus was also elevated in the dynamic bone histomorphometry at week 8 in OVX rats treated with Scl-Ab. The increase in MS/BS, BFR/BS and MAR at the periosteal callus region in the OVX-Scl-Ab group indicated an increased bone matrix deposited per active osteoblast cluster and recruitment of osteoblasts during remodelling compared with the OVX–Saline group. Our results were consistent with those of Ominsky et al., who showed that Scl-Ab could enhance the bone mass in a rat fracture model after treatment with Scl-Ab for 7 weeks [29], and also showed that treatment with Scl-Ab for 8 weeks could enhance the bone mass in OVX rats with a fracture. Furthermore, it has been reported that the deterioration of bone architecture could be implicated in the decrease in bone strength and increase of the prevalence of fractures in humans [31]. In our study, the increased bone mass in the callus of Scl-Ab-treated OVX rats corresponded to a significant increase in maximal loading, energy to maximal loading and stiffness compared with those in the OVX–Saline control group, as shown in Fig. 2. Li et al. reported that treatment with Scl-AbII helped to increase bone strength in ageing OVX rats [6], and Ominsky et al. showed increased bone strength in rats with a fracture after Scl-Ab treatment [29]. Our study further proved that Scl-Ab can help to increase bone strength at the fracture region in OVX rats. Our data did not show a significant difference between the OVX–Saline and Sham–Saline groups in the mechanical properties at the fracture region at week 8. In the study conducted by Mitsuru Saito, ovariectomy was reported to be responsible for the decrease in stiffness during fracture healing as stiffness was only significantly decreased in the OVX group compared with sham group at week 12 [32]. In the normal femoral midshaft, Li and colleagues also showed that only stiffness was significantly increased in sham rats compared with OVX rats 12 months later after ovariectomy [6]. Our data further showed no significant difference in mechanical properties between the Sham–Saline and OVX–Saline groups at an earlier time of week 8 during fracture healing. The significant difference on the mechanical properties at the fracture site between OVX–Saline and Sham–Saline rats may happen in a longer time. Patients with an initial osteoporotic fracture are at a greater risk of secondary osteoporotic fractures [33]. Therefore, treatment with Scl-Ab of patients with osteoporotic fractures could help to increase bone mass, bone strength and bone formation at the fracture region. This has significant implications for the clinical potential of sclerostin inhibition on osteoporotic fracture healing, especially for older women with a high prevalence fractures due to postmenopausal osteoporosis.

Wnt signalling pathways play an important role in bone development, bone formation and bone growth [8–10]. Sclerostin is mainly expressed on osteocytes and inhibits bone formation by antagonising the Wnt signalling pathway [6, 12, 13]. Moreover, BMSCs are multipotent cells that arise from the mesenchyme during development and possess an extensive potential to proliferate and differentiate into osteoblasts [34]. To study the underlying mechanism of Scl-Ab on fracture healing in OVX rats further, we also isolated the BMSCs at week 8 after treatment. The results showed that more CFUs and ALP^+ CFUs were observed in the OVX-Scl-Ab group than in the OVX–Saline and Sham–Saline groups, respectively. The increased colony number indicated that more mononuclear cells were recruited from bone marrow (which contains bone-forming precursor cells) to differentiate into osteoblasts and further helped to promote bone formation in the OVX-Scl-Ab group. The ALP positive colonies were considered as bone-forming progenitor cells. As ALP is a by-product of osteoblast activity, the elevated ALP^+ colonies implied that active bone formation may occur in the OVX-Scl-Ab group [35]. This is also associated with the observed increased mineralising surface (MS/BS) in the OVX-Scl-Ab group in our study. Sutherland and colleagues also showed that sclerostin can decrease the osteoblast activity and reduce the differentiation of osteoprogenitors in human mesenchymal stem cells [36]. Sclerostin also competed with type I and type II bone morphogenetic protein (BMP) receptors for binding to BMPs, which may lead to decreased BMP signalling and suppressed mineralisation of osteoblastic cells [37]. These findings may further explain why the increase in BMSCs may have helped to promote fracture healing in Scl-Ab-treated OVX rats in our study.

Angiogenesis is an essential stage during bone healing, especially during the early stage of fracture healing. Previous studies also demonstrated that angiogenic factors, such as vascular endothelial growth factor, were required during bone healing [38, 39]. In our study, we compared the vessel formation at the fracture region in each group at week 8 after the fracture by micro-CT analysis. The 3D reconstruction images showed that less obvious structures of vessel network were formed in each group. The measurements of vessel volume and vessel fraction were lower in OVX-Scl-Ab group than that of the OVX–Saline group, but there is no significant difference. An early time point to examine the angiogenesis status will be carried out in our future study [40].

There were also limitations in our study. We only studied the effects of Scl-Ab on fracture healing in OVX rats at week 8. An earlier time point before week 8 could also be chosen to study the fracture healing process further, such as comparing the dynamic bone formation and angiogenesis. In addition, our study showed more CFUs in

BMSCs isolated from Scl-Ab-treated OVX rats, but the underlying mechanisms remain unknown and are worthy of further investigation.

In summary, we examined the effects of the subcutaneous injection of Scl-Ab on fracture healing in ovariectomised rats. Our results demonstrated that Scl-Ab enhanced fracture healing in OVX rats by improving bone mass, bone strength and bone formation at the fracture region. Overall, these results suggested that Scl-Ab may have a potential benefit in healing osteoporotic fractures.

Acknowledgments We thank Amgen Inc. and UCB Pharma who provided funding and Scl-Ab for this study. This work was supported by a Grant from the Hong Kong Government Research Grant Council, General Research Fund (CUHK470813) and a Grant from China Shenzhen City Science and Technology Bureau under the Shenzhen City Knowledge Innovation Plan, Basic Research Project (JCYJ20130401171935811) to Gang Li. This study was also supported in part by the SMART program, Lui Che Woo Institute of Innovative Medicine, Faculty of Medicine, The Chinese University of Hong Kong. This research project was made possible by resources donated by Lui Che Woo Foundation Limited.

Compliance with Ethical Standards

Conflicts of Interest Yang Liu, Yunfeng Rui, Tin Yan Cheng, Shuo Huang, Liangliang Xu, Fanbiao Meng, Wayne Yuk Wai Lee, Ting Zhang, Nan Li, Chaoyang Li, Huazhu Ke and Gang Li declare that they have no conflict of interest.

Human and Animal Rights and Informed Consent All animal experiments were approved by the Animal Experimentation Ethics Committee of The Chinese University of Hong Kong, Hong Kong, China.

References

1. Cummings SR, Melton LJ (2002) Epidemiology and outcomes of osteoporotic fractures. Lancet 359(9319):1761–1767
2. Johnell O, Kanis J (2005) Epidemiology of osteoporotic fractures. Osteoporos Int 16(Suppl 2):S3–S7
3. Ke HZ et al (2012) Sclerostin and Dickkopf-1 as therapeutic targets in bone diseases. Endocr Rev 33(5):747–783
4. McKibbin B (1978) The biology of fracture healing in long bones. J Bone Joint Surg Br 60-B(2):150–162
5. Frost HM (1989) The biology of fracture healing. An overview for clinicians. Part I. Clin Orthop Relat Res 248:283–293
6. Li X et al (2009) Sclerostin antibody treatment increases bone formation, bone mass, and bone strength in a rat model of postmenopausal osteoporosis. J Bone Miner Res 24(4):578–588
7. Ring D et al (2004) Locking compression plates for osteoporotic nonunions of the diaphyseal humerus. Clin Orthop Relat Res 425:50–54
8. Hill TP et al (2005) Canonical Wnt/beta-catenin signaling prevents osteoblasts from differentiating into chondrocytes. Dev Cell 8(5):727–738
9. Hoeppner LH, Secreto FJ, Westendorf JJ (2009) Wnt signaling as a therapeutic target for bone diseases. Expert Opin Ther Targets 13(4):485–496
10. Komatsu DE et al (2010) Modulation of Wnt signaling influences fracture repair. J Orthop Res 28(7):928–936
11. Zhang R et al (2013) Wnt/beta-catenin signaling activates bone morphogenetic protein 2 expression in osteoblasts. Bone 52(1):145–156
12. Kamiya N et al (2008) BMP signaling negatively regulates bone mass through sclerostin by inhibiting the canonical Wnt pathway. Development 135(22):3801–3811
13. Krishnan V, Bryant HU, Macdougald OA (2006) Regulation of bone mass by Wnt signaling. J Clin Invest 116(5):1202–1209
14. Ten Dijke P et al (2008) Osteocyte-derived sclerostin inhibits bone formation: its role in bone morphogenetic protein and Wnt signaling. J Bone Joint Surg Am 90(Suppl 1):31–35
15. Van Bezooijen RL et al (2007) Wnt but not BMP signaling is involved in the inhibitory action of sclerostin on BMP-stimulated bone formation. J Bone Miner Res 22(1):19–28
16. Brunkow ME, Gardner JC, Van Ness J, Paeper BW, Kovacevich BR (2001) Bone dysplasia sclerosteosis results from loss of the SOST gene product, a novel cystine knot-containing protein. Am J Hum Genet 68:577–589
17. Balemans W, Ebeling M, Patel N (2001) Increased bone density in sclerosteosis is due to the deficiency of a novel secreted protein (SOST). Hum Mol Genet 10(5):537–543
18. Kramer I et al (2010) Parathyroid hormone (PTH)-induced bone gain is blunted in SOST overexpressing and deficient mice. J Bone Miner Res 25(2):178–189
19. McDonald MM et al (2012) Inhibition of sclerostin by systemic treatment with sclerostin antibody enhances healing of proximal tibial defects in ovariectomized rats. J Orthop Res 30(10):1541–1548
20. Padhi D et al (2011) Single-dose, placebo-controlled, randomized study of AMG 785, a sclerostin monoclonal antibody. J Bone Miner Res 26(1):19–26
21. Bonnarens Frank, Einhorn TA (1984) Production of a standard closed fracture in laboratory animal bone. J Orthop Res 2(1):97–102
22. Mittra E et al (2008) Evaluation of trabecular mechanical and microstructural properties in human calcaneal bone of advanced age using mechanical testing, microCT, and DXA. J Biomech 41(2):368–375
23. Suen PK et al (2014) Sclerostin monoclonal antibody enhanced bone fracture healing in an open osteotomy model in rats. J Orthop Res 32(8):997–1005
24. Dempster DW et al (2013) Standardized nomenclature, symbols, and units for bone histomorphometry: a 2012 update of the report of the ASBMR Histomorphometry Nomenclature Committee. J Bone Miner Res 28(1):2–17
25. He YX et al (2011) Impaired bone healing pattern in mice with ovariectomy-induced osteoporosis: a drill-hole defect model. Bone 48(6):1388–1400
26. He YX et al (2012) Deletion of estrogen receptor beta accelerates early stage of bone healing in a mouse osteotomy model. Osteoporos Int 23(1):377–389
27. Xu L et al (2012) Cellular retinol-binding protein 1 (CRBP-1) regulates osteogenenesis and adipogenesis of mesenchymal stem cells through inhibiting RXRalpha-induced beta-catenin degradation. Int J Biochem Cell Biol 44(4):612–619
28. Augat P et al (2005) Mechanics and mechano-biology of fracture healing in normal and osteoporotic bone. Osteoporos Int 16(Suppl 2):S36–S43
29. Ominsky MS et al (2011) Inhibition of sclerostin by monoclonal antibody enhances bone healing and improves bone density and strength of nonfractured bones. J Bone Miner Res 26(5):1012–1021
30. Padhi D, Stouch B, Jang G, Fang L, Darling M, Glise H, Robinson M, Harris S, Posvar E (2007) Anti-sclerostin antibody increases markers of bone formation in healthy postmenopausal women. J Bone Miner Res S1:S37
31. Hamann C et al (2013) Sclerostin antibody treatment improves bone mass, bone strength, and bone defect regeneration in rats with type 2 diabetes mellitus. J Bone Miner Res 28(3):627–638

32. Saito M et al (2010) Comparison of effects of alfacalcidol and alendronate on mechanical properties and bone collagen cross-links of callus in the fracture repair rat model. Bone 46(4):1170–1179
33. Center JR, Bliuc D, Nguyen TV, Eisman JA (2007) Risk of subsequent fracture after low trauma fracture in men and women. JAMA 297(4):387–394
34. Heino TJ, Hentunen TA (2008) Differentiation of osteoblasts and osteocytes from mesenchymal stem cells. Curr Stem Cell Res Ther 3(2):131–145
35. Farley JR, Baylink DJ (1986) Skeletal alkaline phosphatase activity as a bone formation index in vitro. Metabolism 35(6):563–572
36. Sutherland MK et al (2004) Sclerostin promotes the apoptosis of human osteoblastic cells: a novel regulation of bone formation. Bone 35(4):828–835
37. Winkler DG, Sutherland MK, Geoghegan JC (2003) Osteocyte control of bone formation via sclerostin. EMBO J 22(23):6267–6276
38. Jacobsen KA et al (2008) Bone formation during distraction osteogenesis is dependent on both VEGFR1 and VEGFR2 signaling. J Bone Miner Res 23(5):596–609
39. Street J et al (2002) Vascular endothelial growth factor stimulates bone repair by promoting angiogenesis and bone turnover. Proc Natl Acad Sci USA 99(15):9656–9661
40. Lu C, Marcucio R, Miclau T (2006) Assessing angiogenesis during fracture healing. Iowa Orthop J 26:17–26